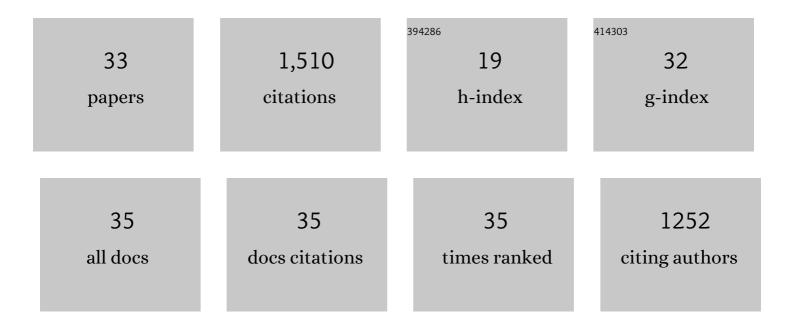
## Yaxue Dong

List of Publications by Year in descending order

Source: https://exaly.com/author-pdf/8852430/publications.pdf

Version: 2024-02-01



YAYUE DONG

#	Article	IF	CITATIONS
1	Discrete Aurora on the Nightside of Mars: Occurrence Location and Probability. Journal of Geophysical Research: Space Physics, 2022, 127, .	0.8	6
2	Energetic Neutral Atoms near Mars: Predicted Distributions Based on MAVEN Measurements. Astrophysical Journal, 2022, 927, 11.	1.6	2
3	Particleâ€In ell Modeling of Martian Magnetic Cusps and Their Role in Enhancing Nightside Ionospheric Ion Escape. Geophysical Research Letters, 2021, 48, .	1.5	7
4	Mars Dust Storm Effects in the Ionosphere and Magnetosphere and Implications for Atmospheric Carbon Loss. Journal of Geophysical Research: Space Physics, 2020, 125, no.	0.8	23
5	Influence of the Solar Wind Dynamic Pressure on the Ion Precipitation: MAVEN Observations and Simulation Results. Journal of Geophysical Research: Space Physics, 2020, 125, e2020JA028183.	0.8	6
6	Characterizing Mars's Magnetotail Topology With Respect to the Upstream Interplanetary Magnetic Fields. Journal of Geophysical Research: Space Physics, 2020, 125, no.	0.8	21
7	The global current systems of the Martian induced magnetosphere. Nature Astronomy, 2020, 4, 979-985.	4.2	55
8	Influence of Extreme Ultraviolet Irradiance Variations on the Precipitating Ion Flux From MAVEN Observations. Geophysical Research Letters, 2019, 46, 7761-7768.	1.5	5
9	Mars Upper Atmospheric Responses to the 10 September 2017 Solar Flare: A Global, Timeâ€Dependent Simulation. Geophysical Research Letters, 2019, 46, 9334-9343.	1.5	19
10	Magnetic Field in the Martian Magnetosheath and the Application as an IMF Clock Angle Proxy. Journal of Geophysical Research: Space Physics, 2019, 124, 4295-4313.	0.8	16
11	Spatial variations in the dust-to-gas ratio of Enceladus' plume. Icarus, 2018, 305, 123-138.	1.1	15
12	The Morphology of the Solar Wind Magnetic Field Draping on the Dayside of Mars and Its Variability. Geophysical Research Letters, 2018, 45, 3356-3365.	1.5	39
13	A Proxy for the Upstream IMF Clock Angle Using MAVEN Magnetic Field Data. Journal of Geophysical Research: Space Physics, 2018, 123, 9612-9618.	0.8	6
14	An Artificial Neural Network for Inferring Solar Wind Proxies at Mars. Geophysical Research Letters, 2018, 45, 10,855.	1.5	21
15	Loss of the Martian atmosphere to space: Present-day loss rates determined from MAVEN observations and integrated loss through time. Icarus, 2018, 315, 146-157.	1.1	216
16	Seasonal variability of Martian ion escape through the plume and tail from MAVEN observations. Journal of Geophysical Research: Space Physics, 2017, 122, 4009-4022.	0.8	66
17	The Mars crustal magnetic field control of plasma boundary locations and atmospheric loss: MHD prediction and comparison with MAVEN. Journal of Geophysical Research: Space Physics, 2017, 122, 4117-4137.	0.8	60
18	Statistical analysis of the reflection of incident O <sup>+</sup> pickup ions at Mars: MAVEN observations. Journal of Geophysical Research: Space Physics, 2017, 122, 4089-4101.	0.8	11

YAXUE DONG

#	Article	IF	CITATIONS
19	O <sup>+</sup> ion beams reflected below the Martian bow shock: MAVEN observations. Journal of Geophysical Research: Space Physics, 2016, 121, 3093-3107.	0.8	13
20	Space Weather Storm Responses at Mars: Lessons from A Weakly Magnetized Terrestrial Planet. Proceedings of the International Astronomical Union, 2016, 12, 211-217.	0.0	0
21	Response of Mars O <sup>+</sup> pickup ions to the 8 March 2015 ICME: Inferences from MAVEN dataâ€based models. Geophysical Research Letters, 2015, 42, 9095-9102.	1.5	47
22	Control of Mars global atmospheric loss by the continuous rotation of the crustal magnetic field: A timeâ€dependent MHD study. Journal of Geophysical Research: Space Physics, 2015, 120, 10,926.	0.8	61
23	Strong plume fluxes at Mars observed by MAVEN: An important planetary ion escape channel. Geophysical Research Letters, 2015, 42, 8942-8950.	1.5	143
24	Multifluid MHD study of the solar wind interaction with Mars' upper atmosphere during the 2015 March 8th ICME event. Geophysical Research Letters, 2015, 42, 9103-9112.	1.5	54
25	MHD model results of solar wind interaction with Mars and comparison with MAVEN plasma observations. Geophysical Research Letters, 2015, 42, 9113-9120.	1.5	58
26	Characteristics of ice grains in the Enceladus plume from Cassini observations. Journal of Geophysical Research: Space Physics, 2015, 120, 915-937.	0.8	34
27	The spatial distribution of planetary ion fluxes near Mars observed by MAVEN. Geophysical Research Letters, 2015, 42, 9142-9148.	1.5	115
28	Modeling the total dust production of Enceladus from stochastic charge equilibrium and simulations. Planetary and Space Science, 2015, 119, 208-221.	0.9	10
29	MAVEN observations of the response of Mars to an interplanetary coronal mass ejection. Science, 2015, 350, aad0210.	6.0	166
30	Early MAVEN Deep Dip campaign reveals thermosphere and ionosphere variability. Science, 2015, 350, aad0459.	6.0	90
31	A model of the spatial and size distribution of Enceladus× <sup>3</sup> dust plume. Planetary and Space Science, 2014, 104, 216-233.	0.9	15
32	Charged nanograins in the Enceladus plume. Journal of Geophysical Research, 2012, 117, .	3.3	71
33	The water vapor plumes of Enceladus. Journal of Geophysical Research, 2011, 116, n/a-n/a.	3.3	39